

Section 2

ADVANCED TECHNOLOGY DEVELOPMENTS

2.A Transparent Conductive Coating of KDP Using Ion-Assisted Deposition

Several types of electro-optic devices require electrodes that are both optically transparent and electrically conductive. Examples of such devices useful for inertial fusion lasers are given in Table 43.I. Some devices, such as the longitudinal Pockels cell, require application of a transparent electrode to a thermally sensitive substrate of potassium dihydrogen phosphate (KDP). The applied coating must also have a high laser-damage threshold for the infrared (1054 nm). A variety of methods¹ have been developed for depositing transparent conductors, but most require heating the substrate to promote complete oxidation of the film. This article describes a technique for depositing transparent conductors using indium-tin oxide (ITO) with ion-assisted deposition (IAD).

Both thin metal films and oxide semiconductors have been used for transparent conductors. Metal films have high absorption, hence, a correspondingly low laser-damage threshold, making them unsuitable for the applications listed in Table 43.I. The high transparency of the oxide-semiconductor films derives from their high band gap energy, i.e., > 3.0 eV. Optical losses in the films have two origins: (1) interfacial reflection losses caused by refractive index mismatch to the substrate and incident media; and (2) absorption losses caused by non-stoichiometric films or impurities introduced to induce conduction. The first loss mechanism may be compensated for by appropriate optical-thin-film design. The second mechanism must be balanced against the need for low electrical resistance.

Table 43.I: Transparent conductor requirements for devices used in high-energy lasers.

Device	High Transparency	Low Resistance	High Fluence	Thermal Limits
Profile-tunable liquid crystal laser aperture ²	X			X
Liquid crystal beam steering and switching	X	X		
Longitudinal-mode KDP Pockels cell	X	X	X	X

G2947

In addition, an abundance of free carriers (electrons) in the film can produce a plasma resonance peak in the infrared (for ITO this is about 1.5 μm). At infrared wavelengths longer than this absorption peak the coating will be highly reflective.

The intrinsic conductivity σ of a material is directly related to the carrier density N , carrier mobility μ , and the carrier charge e , such that $\sigma = Ne\mu$. Conduction in oxides may be enhanced by the introduction of free carriers into the lattice. These carriers may originate either from a departure from the stoichiometric oxide or by the introduction of impurity (dopant) atoms into the lattice. In this work we use indium oxide (In_2O_3) doped with tin giving an N -type conductivity. Both the high-valence tin and the oxygen vacancies contribute to conductivity in ITO. Carrier mobility also has a significant effect on conductivity. The mobility in a transparent conductor is impeded by scatter from grain boundaries, ionized impurities, and the interfaces. All of these mechanisms contribute to a low mobility in the thin-film form when compared to the bulk material.

A complex picture forms when the realities of the thin-film process are considered. A change in a single-process parameter, such as substrate temperature, evaporation rate, or oxygen backfill pressure, can simultaneously alter film stoichiometry and structure. Independent control of carrier density and mobility can therefore be very difficult. If temperature control is removed by substrate constraints, it is not possible to obtain stoichiometric films since oxidation is incomplete at the film surface. Ion-assisted deposition (Fig. 43.22) can provide the additional control by bombarding the substrate with relatively high-energy ions (with respect to the low thermal energy of the evaporant). By controlling the ion energy and flux, significant changes in the film structure can be induced.^{3,4} If the ion

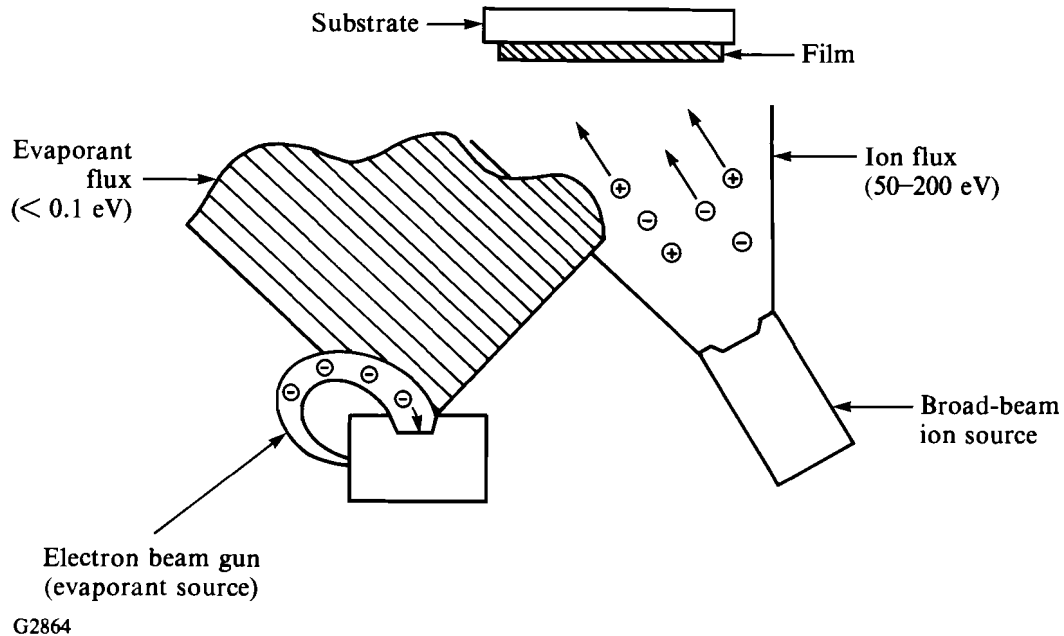


Fig. 43.22

Schematic of ion-assisted deposition. The low-energy evaporant flux is given additional kinetic energy by the high-energy ions at the film formation surface. An inert or reactive gas (such as oxygen) may be used for the ion flux. Oxygen, which was used for the ITO coatings, promotes oxidation at the interface if it is not too energetic.

is a reactive species, such as oxygen, the stoichiometry may also be affected by both implantation and preferential sputtering.

Coatings with high laser-damage thresholds generally must have low absorption at the laser wavelength. However, transparent conductors will have some absorption (due to free carriers), but it can be minimized by increasing conductivity with higher carrier mobility. IAD is used to control the grain size and the stoichiometry while maintaining the substrate at near-ambient temperature. This method is used to coat KDP with a transparent conductor of ITO. Holding the KDP at a temperature close to ambient avoids deleterious effects caused by the differential expansion coefficients of KDP.⁵

Experimental Procedure

1. Deposition-chamber geometry

The ITO coatings were produced in a 28-in.-diam cylindrical vacuum chamber. The chamber contains an electron-beam evaporation source and an 8-cm-aperture broad-beam ion source, which are placed approximately 50 cm and 40 cm below the substrate mount, respectively. The ion source has a dual graphite-accelerator grid that is designed to produce a collimated beam of monoenergetic ions.⁶ The impingement rate of the ions is measured

by a negatively biased Faraday cup probe located at the height of the substrate mount. Deposition rate of the evaporant mass was monitored by a resonating quartz crystal sensor. A thermocouple located near the substrate holder monitored the changes in ambient temperature of the chamber during the deposition.

The substrates were rotated to obtain better time-averaged uniformity of both the evaporant and the ion source. The ion source was pointed approximately 6 cm away from the center of the substrate rotation⁴ to obtain the optimum uniformity of both quantities.

The chamber is evacuated by a cryogenic pump to pressures less than 4×10^{-6} mBar prior to depositions. Continuous addition of oxygen gas through the ion source raises the chamber pressure to 1×10^{-4} mBar during the evaporation. Deposition rate of the ITO evaporant was fixed at 0.1 nm/s for all experiments, and the substrate rotation was kept at 6.6 rpm. All substrates were precleaned for 2 min with 500-eV Ar⁺ ions at an impingement rate of $\sim 40 \mu\text{A}/\text{cm}^2$ prior to the onset of film deposition. This step is employed to remove impurities that can hinder the film-substrate adhesion. Following this step, the ion-source parameters were adjusted for subsequent operation with oxygen gas.

2. Characterization

The conductivity of a thin film is often expressed in terms of sheet resistance R_{sh} with units ohms per square (Ω/sq), which is related to the inherent film resistivity ρ and thickness d by

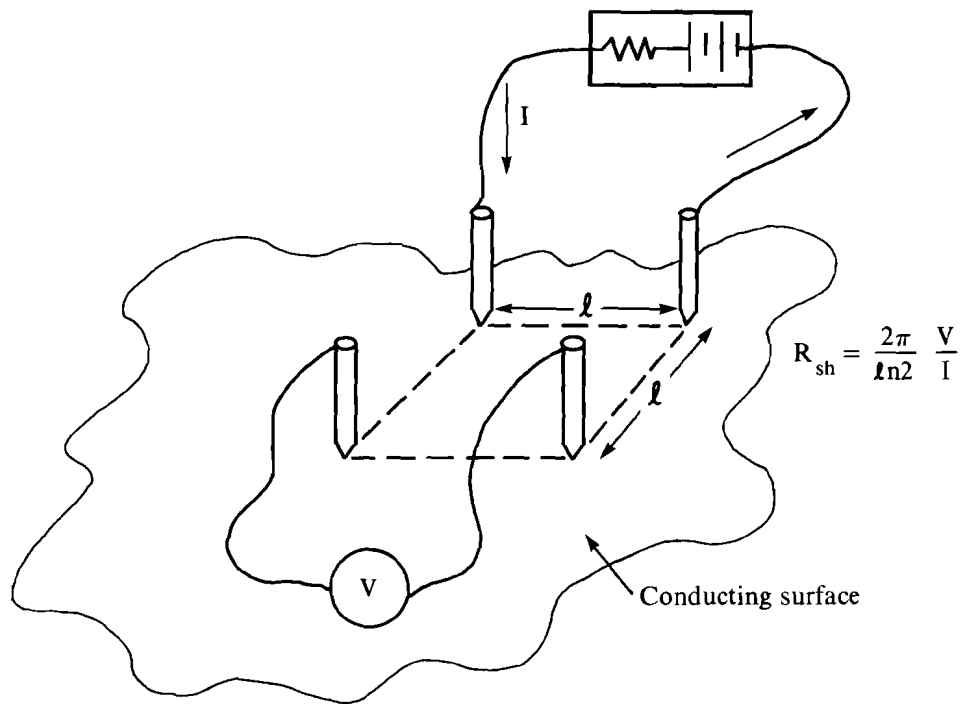
$$R_{\text{sh}} = \frac{\rho}{d}. \quad (1)$$

A four-point square-contact probe, illustrated in Fig. 43.23, is used to measure this quantity. After bringing the probe tips in contact with the film surface, a known amount of current is allowed to flow through two adjacent tips, and the voltage generated across the other two tips is measured. The sheet resistance value is then determined from these two quantities with the equation⁷

$$R_{\text{sh}} = \frac{2\pi}{\ln 2} \frac{V}{I} = 9.06 \frac{V}{I}. \quad (2)$$

The measurement error introduced by physical deviation of the probe from its square design can be determined by averaging measurements from all parallel combinations of current path and voltage measurement.

Optical transparency of the coatings was measured in the wavelength range from 0.3 μm to 25 μm . Figure 43.24 shows some typical results in the visible and near infrared, while the spectrum for 2.5 μm to 25 μm is seen in Fig. 43.25.



G2936

Fig. 43.23
 A four-point square-contact probe apparatus used to measure the sheet resistances of ITO coatings. Only the measurement accuracy is dependent on the size of the square ℓ .

As stated above, the optical and electrical characteristics of transparent conductors are complex functions of numerous quantities (e.g., carrier density and mobility, dopant level, film thickness, and stoichiometry, etc.).^{4,7,8} The uniformity of one of these properties across a film surface does not necessarily suggest the uniformity of the other property. Hence, both the optical transparency and the sheet resistance were measured at several locations across the surface of each film sample throughout the experiments.

Results

After adjustment of several process parameters, a reproducible ITO coating with desired transparency and sheet resistance was produced onto a large substrate area. Transparency of the coatings is relatively insensitive to the changes in deposition parameters within the studied range. However, the conductivity, or conversely the resistivity, of ITO coatings is particularly sensitive to the variations in ion energy and flux for a fixed deposition rate.

Controlled variations in the ion energy and flux produce a significant effect on the properties of ITO coatings. Figure 43.26 shows that film

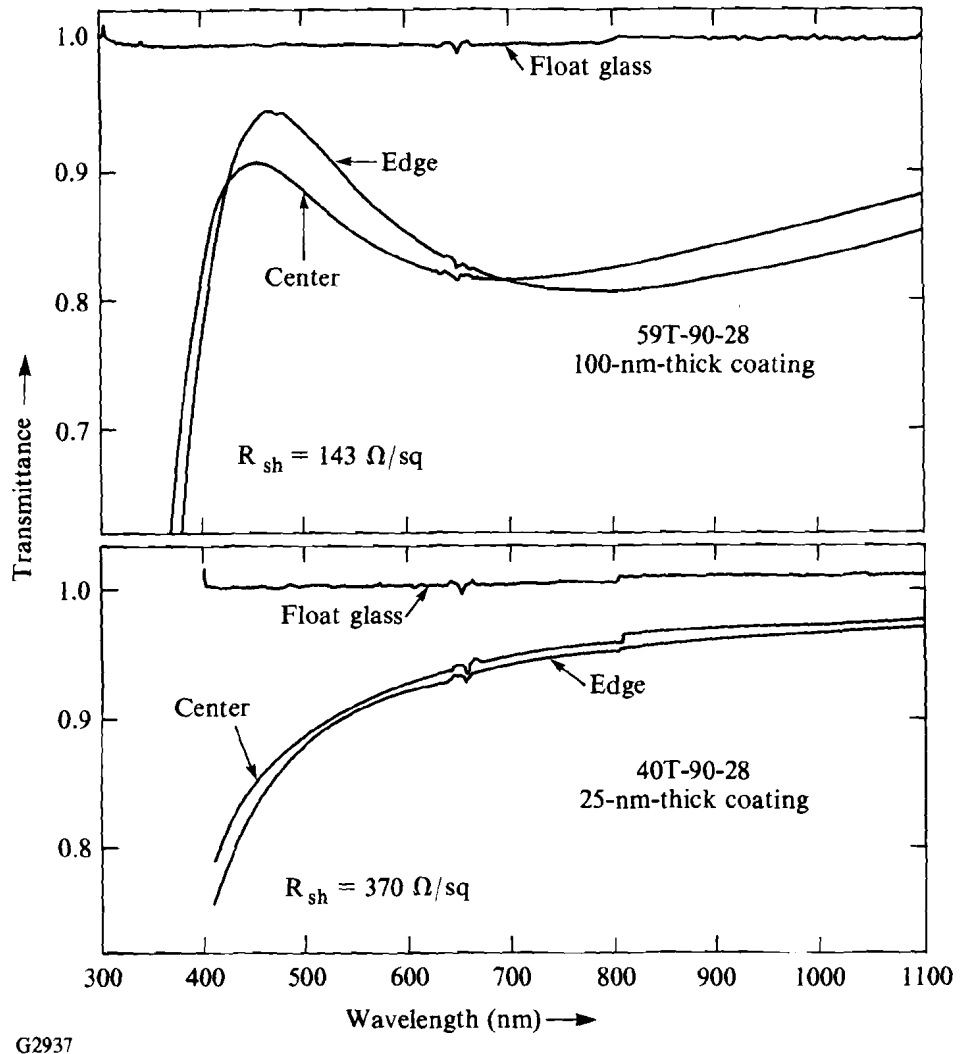


Fig. 43.24 Spectral scans of thick (upper curves) and thin ITO films deposited under optimum IAD conditions at ambient temperatures. The edge pieces were 15 cm from the center of rotation.

resistivity remains at a low constant value for ion energies below 300 eV at a fixed ion-current density. For higher ion energy, a sudden increase in film resistivity occurs. This may have two causes: (1) the film microstructure could be significantly altered, or (2) the higher ion bombardment could produce charge vacancies that act as carrier scatterers. For a fixed ion energy, the resulting film resistivity is particularly sensitive to the ion flux. Figure 43.27 illustrates that < 20% variation in either direction of the optimum ion flux leads to a large increase in film resistivity. From these results, the optimum repeatable ion energy and flux at the substrate for this particular deposition geometry is determined to be 200 eV and $30 \mu\text{A}/\text{cm}^2$, respectively.

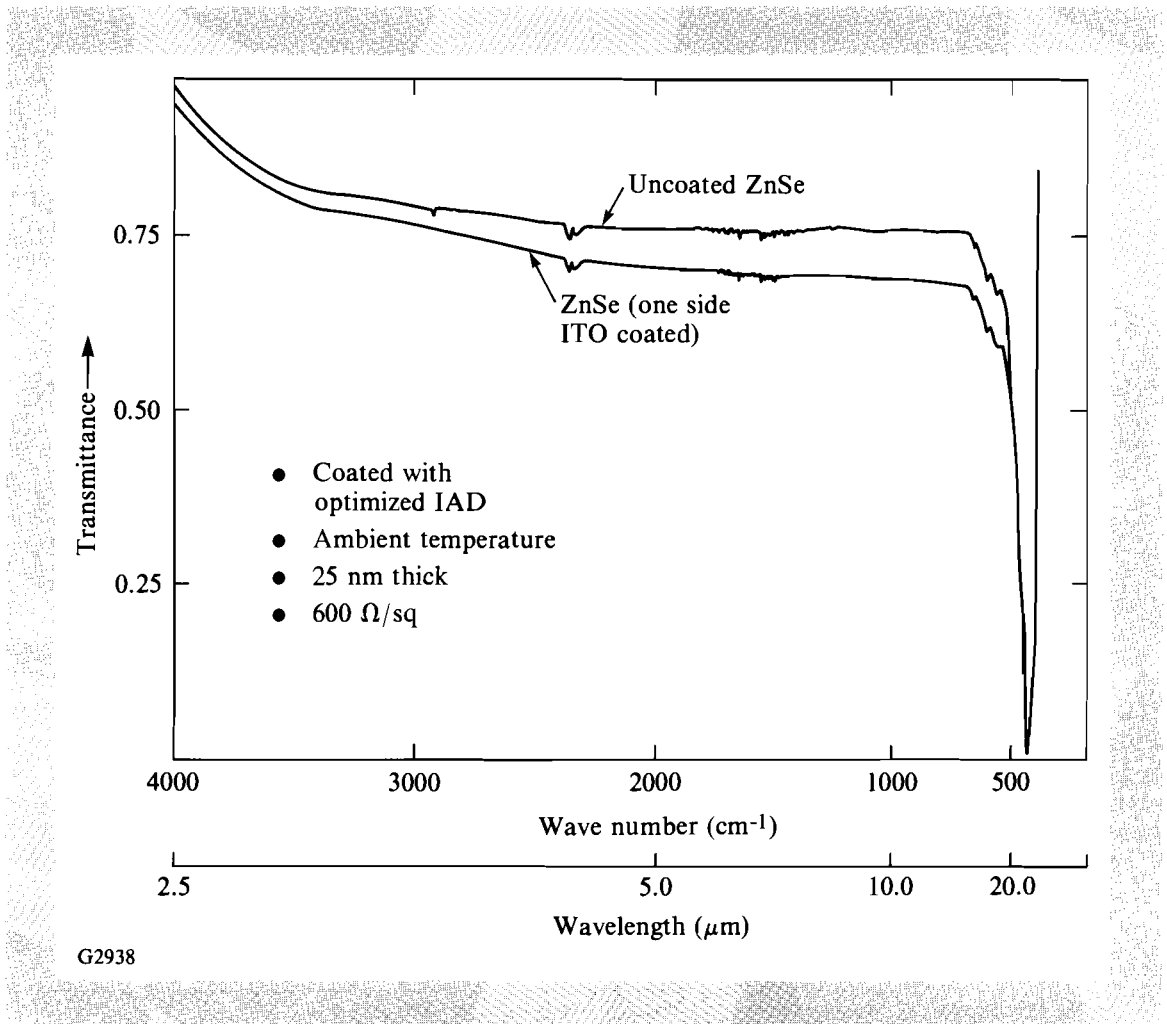


Fig. 43.25

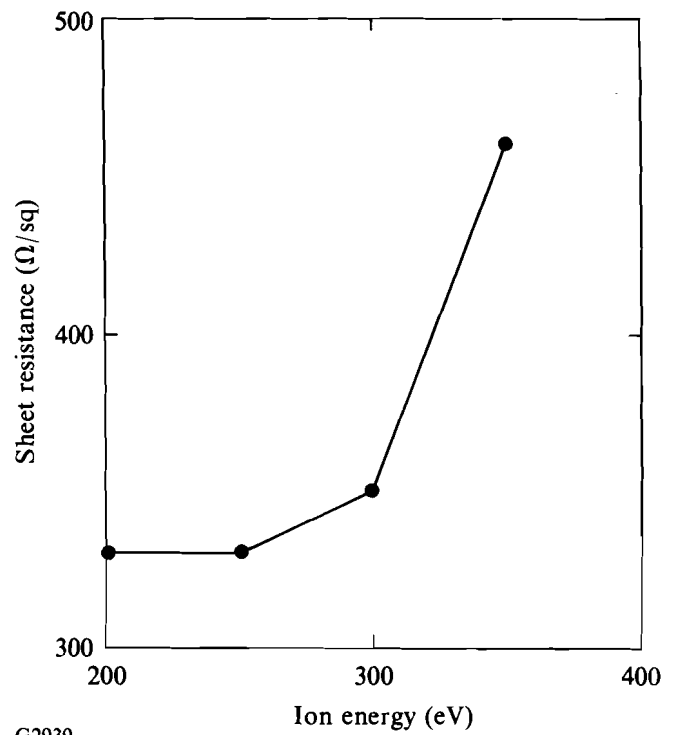
Infrared spectral scan of a thin transparent conductor. The thin coating significantly reduces the strong absorption seen in thicker coatings.

As mentioned in the experimental section, the uniformity of film properties was controlled by varying the ion-source pointing. Figure 43.28 shows that a sheet-resistance uniformity of 12% can ultimately be obtained over a 15-cm diameter after some iterations. The transmission uniformity of films deposited under optimum conditions (Fig. 43.24) is better than 4% across the characterized substrate area. Most film samples exhibit better than 95% transmission in the 0.5- to 25- μ m wavelength range. Adjustment of the ion-source position for optimal sheet-resistance uniformity led to acceptable transmission uniformity since the latter was determined to be far less sensitive to the spatial distribution of average ion flux.

Equation (1) implies that the sheet resistance of ITO coatings should decrease proportionally with increasing film thickness. The measured sheet resistances of several coatings with different thicknesses are plotted in Fig. 43.29 along with the expected sheet resistance curve using the resistivity of

Fig. 43.26

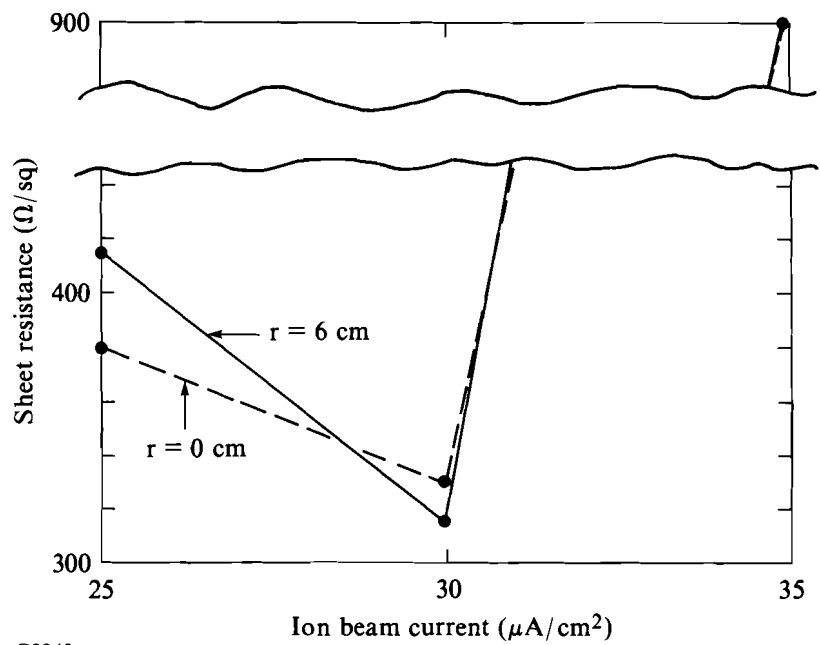
Plot of sheet resistance of ITO coatings as a function of arriving oxygen-ion energy for a fixed ion flux and film thickness. Deposition with 500 eV oxygen-ion assist resulted in nonconducting film.



G2939

Fig. 43.27

Change in sheet resistance of ambient-temperature, IAD-processed ITO coatings obtained by varying ion-beam current at a fixed ion energy (200 eV) and film thickness (25 nm).



G2940

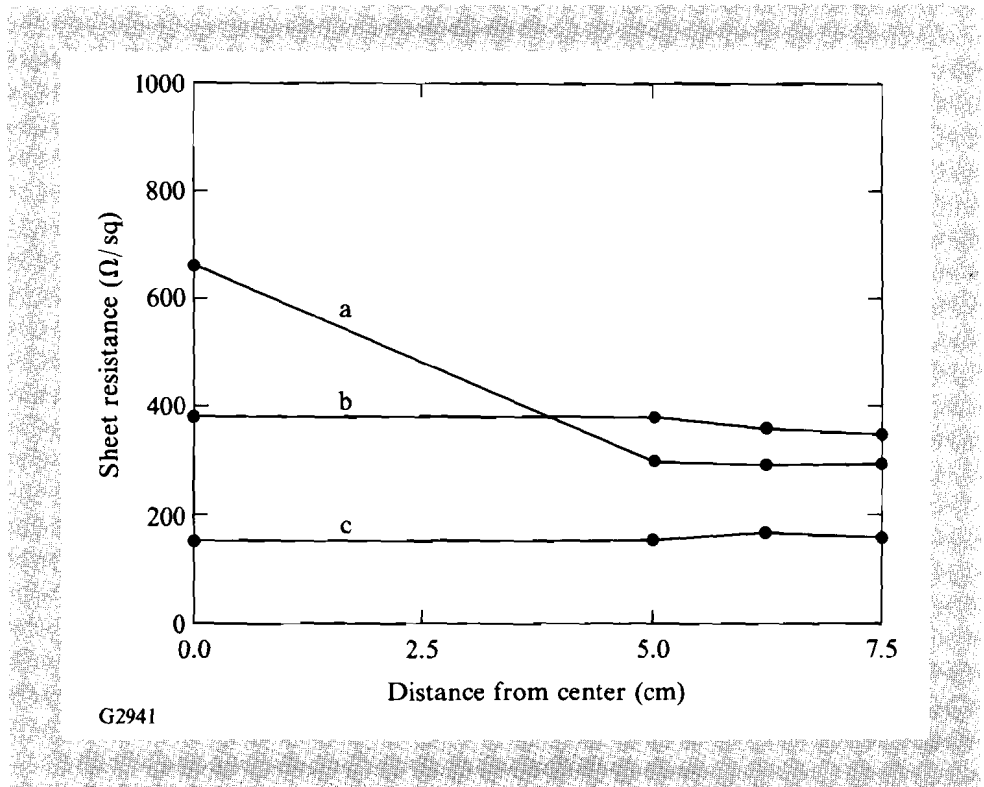


Fig. 43.28 Plot of sheet resistance as a function of radial distance from the center of substrate rotation: (a) before and (b), (c) after optimizing ion-source position. Curve (b) indicates uniformity of thin (25 nm) film, while curve (c) indicates uniformity of 250-nm-thick films.

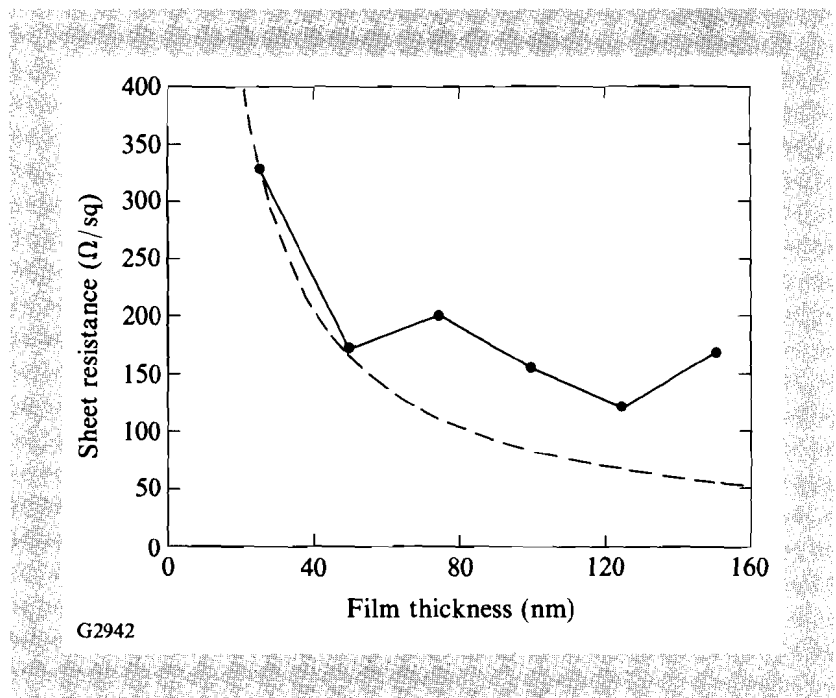
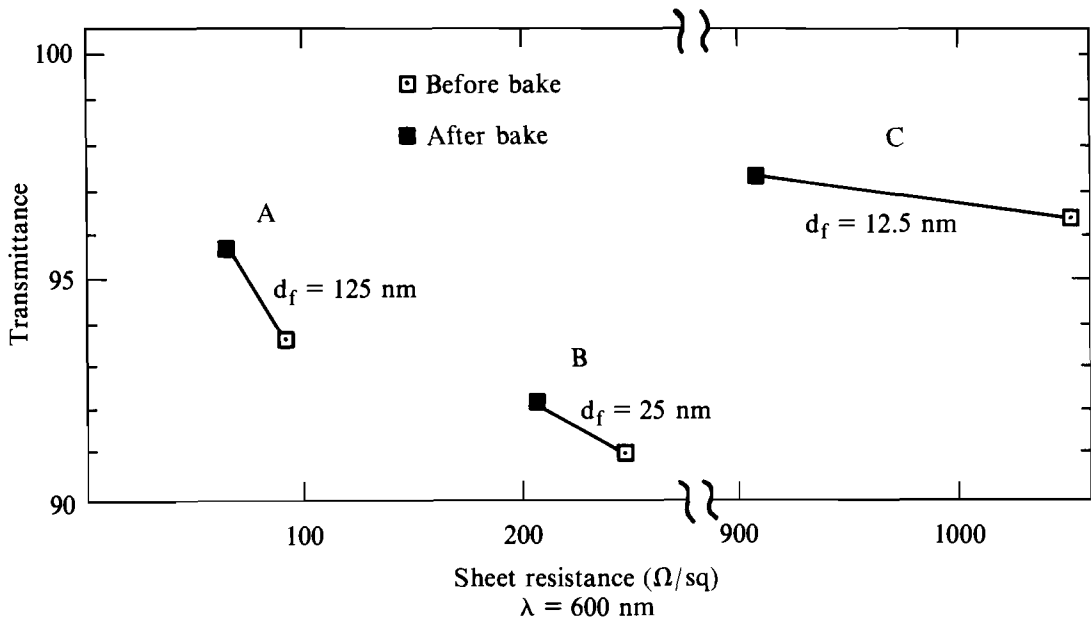


Fig. 43.29 Sheet resistance of ITO coatings deposited under optimized ambient-temperature IAD conditions as a function of film thickness. Dashed curve represents the expected values calculated from resistivity value obtained from 25-nm-thick film.

a 25-nm-thick film. The result indicates that the measured film resistances do not follow the expected thickness dependence. This could be caused by an increase in substrate temperature during the deposition. Thicker films (150 nm) saw a 54°C rise in chamber temperature in contrast to a 25°C rise for a thinner film (25 nm).

Following the initial measurements, several coating samples were baked in atmosphere at temperature gradations from 50°C to 125°C for several hours at each increment and recharacterized. This step was motivated by a conventional ITO deposition procedure that involves post-deposition annealing of films at temperatures above 300°C.¹² Subsequent measurements, summarized in Fig. 43.30, indicate that post-deposition baking induced a noticeable amount of improvement in both transparency and conductivity of the IAD-deposited ITO coatings. The increase in transparency, which is normally observed for heat-treated oxide films deposited in low ambient temperature, can be attributed to improved stoichiometry.⁸ On the other hand, the increase in conductivity is most likely caused by the removal of excess oxygen, which can negate the tin-donor action by trapping carriers, and greater carrier mobility resulting from improved stoichiometry and crystallinity of the host indium oxide.^{1,8,12}



G2943

Fig. 43.30

Increase in transmission and conductivity of ITO coatings observed after 5 h of post-deposition bake at 125°C for films of different thicknesses (d_f) deposited under same IAD conditions.

Conclusion

The ambient-temperature, ion-assisted, electron-beam evaporation process is utilized to produce transparent conducting films of tin-doped indium oxide. Films as thin as 25 nm with better than 95% transmission in the 0.5- to 25- μm wavelength range with sheet resistance less than 350 Ω/sq were uniformly deposited onto a 15-cm-wide substrate area. The ambient temperature of the vacuum chamber did not rise above 54°C even during the deposition of 150-nm-thick films. For conventional reactive evaporation, such results are observed only when the films are deposited onto heated substrates ($T \geq 300^\circ\text{C}$) or annealed at high temperature ($T \geq 400^\circ\text{C}$) following the deposition.^{1,9-12} Comparable values of transparency, sheet resistance, and uniformity are reported by only one other study¹³ that was conducted with a cold-cathode ion source. This process was successfully used to coat small samples of KDP for testing as a longitudinal-mode Pockels cell.

ACKNOWLEDGMENT

This work was supported by the U.S. Department of Energy Division of Inertial Fusion under agreement No. DE-FC03-85DP40200 and by the Laser Fusion Feasibility Project at the Laboratory for Laser Energetics, which has the following sponsors: Empire State Electric Energy Research Corporation, New York State Energy Research and Development Authority, Ontario Hydro, and the University of Rochester.

REFERENCES

1. K. L. Chopra, S. Major, and D. K. Pandya, *Thin Solid Films* **102**, 1 (1983).
2. J. C. Lee, S. D. Jacobs, T. J. Kessler, and N. Van Lieu, "Profile Tunable Laser Beam Apodizer," presented at CLEO '89, Baltimore, MD, 24-28 April 1989.
3. D. J. Smith, C. J. Hayden, B. U. Krakauer, A. W. Schmid, and M. J. Guardalben, *Nat. Bur. Stand. (U.S.) Spec. Publ.* **746**, Laser-Induced Damage in Optical Materials: 1985, 284 (July 1988).
4. M. S. Jin, M.S. thesis, University of Rochester, 1988.
5. "Electro-Optic Properties of KH_2PO_4 and Isomorphous," Cleveland Crystals, Inc., Cleveland, OH.
6. H. R. Kaufman, J. J. Cuomo, and J. M. E. Harper, *J. Vac. Sci. Technol.* **21**, 725 (1982).
7. L. I. Maissel and R. Glang, in *Handbook of Thin Film Technology* (McGraw-Hill, New York, 1970), Chap. 13, pp. 13-1-13-13.
8. J. L. Vossen, *Phys. Thin Films* **9**, 1 (1977).
9. P. J. Martin, R. P. Netterfield, and D. R. McKenzie, *Thin Solid Films* **137**, 207 (1986).